

# Synthesis and Characterization of PVdF/PVP-Based Electrospun Membranes as Separators for Supercapacitor Applications

A. Jabbarnia\* and R. Asmatulu\*

Department of Mechanical Engineering, Wichita State University, 1845 Fairmount, Wichita, KS 67260-0133, US

**Abstract:** Electrospun polyvinylidene fluoride (PVdF)/polyvinylpyrrolidone (PVP) nanofiber embedded with carbon black nanoparticles (<50nm) were fabricated and characterized for supercapacitor separators. Carbon black nanoparticles with different weight percentages (0, 0.25, 0.5, 1, 2, and 4wt%) were added to a mixture of N, N-dimethylacetamide (DMAC)/acetone and sonicated for a well dispersion. Then, PVdF and PVP were added, and the solution was heated on a hot plate to make a polymeric solution prior to the electrospinning process. The morphology of the electrospun nanofibers was characterized by scanning electron microscopy and transmission electron microscopy. Fourier transform infrared spectroscopy was carried out on the PVdF/PVP films to identify changes in the crystalline phase during the process. The annealed nanofibers samples were also examined by X-ray diffraction unit. These investigations demonstrated that the many physical properties were significantly improved, which may be useful for supercapacitor separators. Supercapacitors will become one of the most suitable energy storage devices in the near future, and the separator is one of the major components of the supercapacitors.

**Keywords:** Electrospun Nanofibers, PVdF, carbon black nanopowders, characterization, supercapacitor separators.

## 1. INTRODUCTION

Supercapacitors, ultrasupercapacitors, and electrochemical double-layer capacitors are the most promising energy storage devices with long cyclic functions and high power densities. They have attracted considerable attention because of their low electrical resistivity, large surface area, and superb charging-discharging rate compared to conventional storage devices. They have displayed excellent performance in a wide range of applications such as power backup in some electrical devices and a power source for hybrid vehicles [1-7]. Previous studies have focused on increasing the energy density of supercapacitors by finding suitable materials for the separator/electrode and lowering the overall cost [8]. A large variety of materials, such as metal oxides or materials with carbonaceous compositions such as porous carbon, activated carbon fibers, carbon aerogels, carbon nanotubes, and graphene, are the most frequently used substances in supercapacitors [5-11]. Carbon-based nanocomposites with conducting polymers have high capacitance values and better cyclic performance in supercapacitors. They possess high capacitance values due to their functional groups containing phosphorus, nitrogen, and oxygen, which are referred to as the pseudocapacitance effect [12].

Electrospinning is an effective technique for producing woven and non-woven micro/nanoscale fibers from a polymeric solution. Polymeric separators fabricated by the electrospinning possess a unique texture with micro and/or nanosize fiber arrangements, flexibility, and high surface area and porosity. This can be a promising material for various types of separators. Typically, electrospinning consists of a syringe, syringe pump, high voltage power supply, and collector. The process parameters can be optimized to prepare separators having extraordinary properties. The resultant fibers generally have large surface area, flexibility and uniform porosity [13, 14]. Fibers produced by this method can be used for many industrial applications, such as sensors, filtration, biomedical, reinforcement of composite, solar cells, fuel cells, batteries, supercapacitors, and membrane technology [15, 16].

The main focus of this study was the fabrication and characterization of nanofiber separators for supercapacitors, providing a nanoporous structure resulting in a conductive membrane that can be soaked with liquid electrolyte. Polyvinylidene fluoride polymer was used in this study. Among many polymers, PVdF has shown better results due to its high electrochemical stability and particularly excellent electrical properties, which can be useful for supercapacitor applications, although the flexibility of PVdF is not sufficient due to the high crystallinity of its structure and may eventually, cause some difficulties [17]. PVdF is well known for its polymorphism and, depending on its processing

\*Address correspondence to this author at the Department of Mechanical Engineering, Wichita State University, 1845 Fairmount, Wichita, KS 67260-0133, US; Tel: 001-316-978-6368; Fax: 001-316-978-3236; E-mail: ramazan.asmatulu@wichita.edu, a.jabbarnia@gmail.com

conditions, can display five different polymorphs. PVdF possesses several phases, the most stable and prevalent being the  $\alpha$ -phase (non-polar phase). The important pyroelectric and piezoelectric features of the  $\beta$ -phase (polar phase) of PVdF provide better material properties [18]. The most common technique for transitioning from the non-polar  $\alpha$ -phase to the polar  $\beta$ -phase is with thermal treatment [19]. Electric double-layer (EDL) capacitors prepared with electrospun nonwoven PVdF- polyhexafluoropropylene (PHFP) membrane separators have exhibited excellent cycling efficiency and specific capacity [20].

Carbon black nanopowders are generally used as conductive materials in many types of batteries and supercapacitors. Highly conductive carbon black is described as a highly branched and open structure having a small particle size and high porosity. The specific resistivity of carbon black is typically in the range of  $10^{-1}$  to  $10^{-2}$   $\Omega\text{cm}$ . High porosity and/or finer carbon blacks have more particles per unit weight and, hence, reduce the average inter-aggregate gap width due to their greater number [21]. The surface area of carbon blacks is commonly considered to be more accessible than other types of high surface area carbon [22]. The purpose of this study was to fabricate and

characterize PVdF/PVP separators incorporated with carbon black nanoinclusions for supercapacitors using the electrospinning technique.

## 2. EXPERIMENTAL

### 2.1. Materials

PVdF and PVP with molecular weights of 180,000g/mole and 120,000g/mole, respectively, were purchased from Sigma-Aldrich and used without any modification or purification. Carbon black (ELFTEX8) was purchased from the Cabot Company and used as reinforcement nanoparticles. N, N-dimethylacetamide (DMAC) and acetone were purchased from Fisher Scientific and together used as the solvent. Figure 1 shows SEM and TEM images of carbon black powders used in this experiment. As can be seen, they are mainly aggregated and need to be dispersed well prior to the electrospinning process. TEM images further confirm that the carbon black particles are attached together. The particles have nearly spherical shapes, and the average size is less than 50nm. Agglomerated carbon black powders are observed in the TEM images.

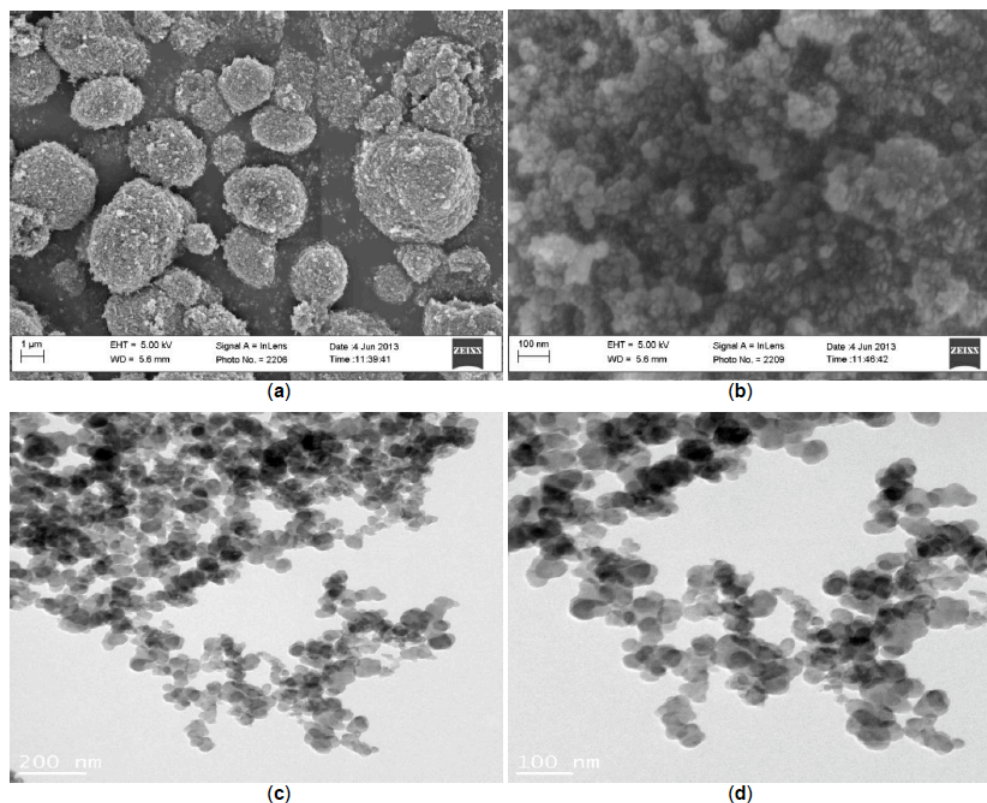


**Figure 1:** (a) SEM image of carbon black powder at low magnification, (b) SEM image of carbon black powder at high magnification, (c) and (d) TEM images of carbon black powder.

## 2.2. Preparation of Electrospun Fibers

Carbon black nanopowders with different weight percentages (0, 0.25, 0.5, 1, 2, and 4wt%) were dispersed in a DMAC/acetone solvent and sonicated for 90 minutes. Then PVdF and 2wt% of PVP were added separately to the dispersions. Ratio of 80:20 was chosen during the dispersion and dissolution processes. The solution was constantly stirred at 550rpm and 60°C for five hours before electrospinning. The dispersed solution was transferred to a 10ml plastic syringe connected to a capillary needle having an inside diameter of 0.5mm. The electrospinning parameters of voltage, distance between tip and collector, and syringe pump speed were 25 kV DC, 25cm, and 2ml/hr, respectively. Electrospun fibers were then collected on an aluminum screen and dried in an

oven at 60°C for eight hours to remove all residual solvents. Electrospun PVdF/PVP fibers were annealed at 90°C for three hours.

## 3. RESULTS AND DISCUSSION

### 3.1. SEM Investigation

The morphology and size distribution of electrospun PVdF/PVP nanofibers were characterized using a field-emission (FE)-SEM instrument (Oxford Instruments, INCA system) equipped with energy-dispersive X-ray (EDX) spectroscopy at an accelerating voltage of 5 and 15 kV. Before SEM observations, the samples were coated with gold spatter. The SEM images of PVdF/PVP nanofibers incorporated with carbon black nanopowders shown in Figure 2 indicate that all PVdF

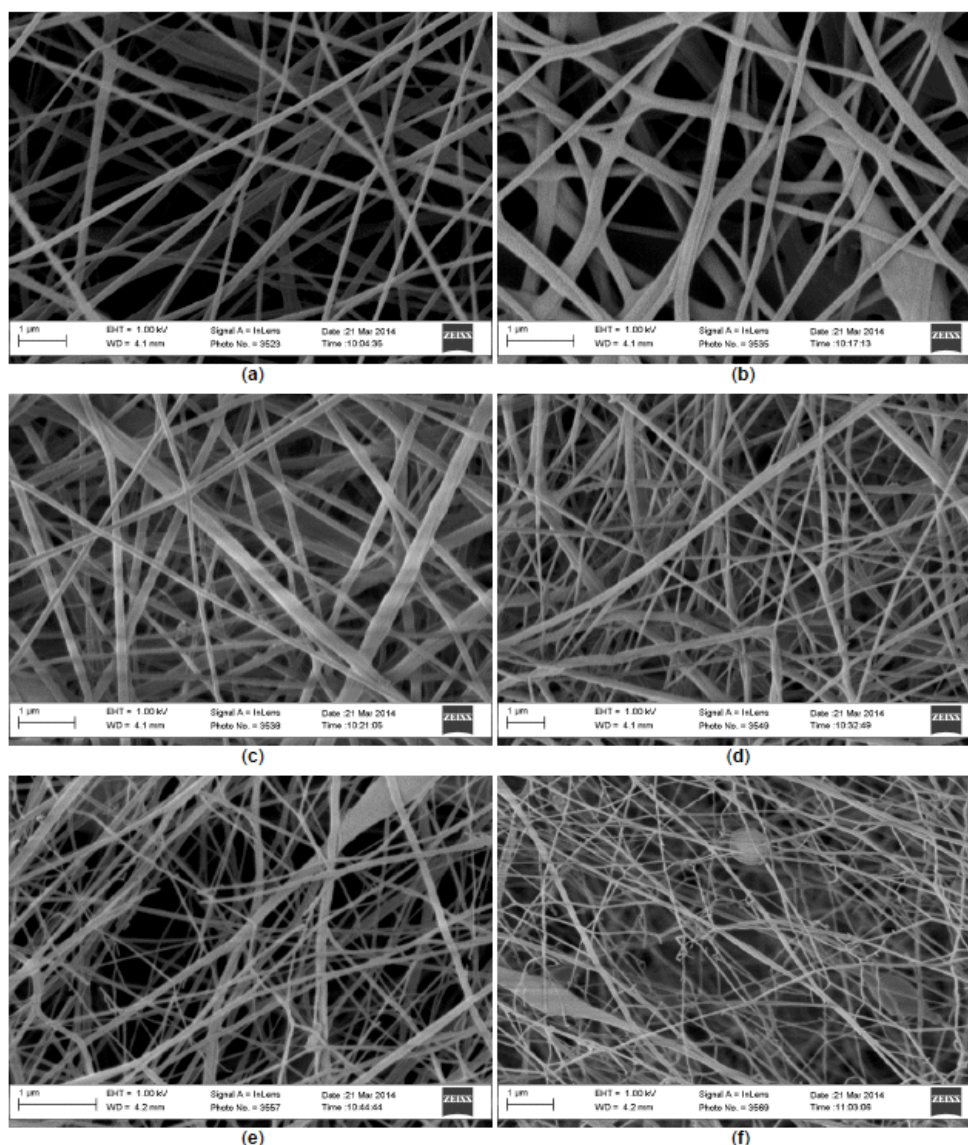


**Figure 2:** SEM images: (a) electrospun PVdF/PVP fibers, and incorporated with (b) 0.25wt%, (c) 0.5wt%, (d) 1wt%, (e) 2wt%, and (f) 4wt% carbon black.

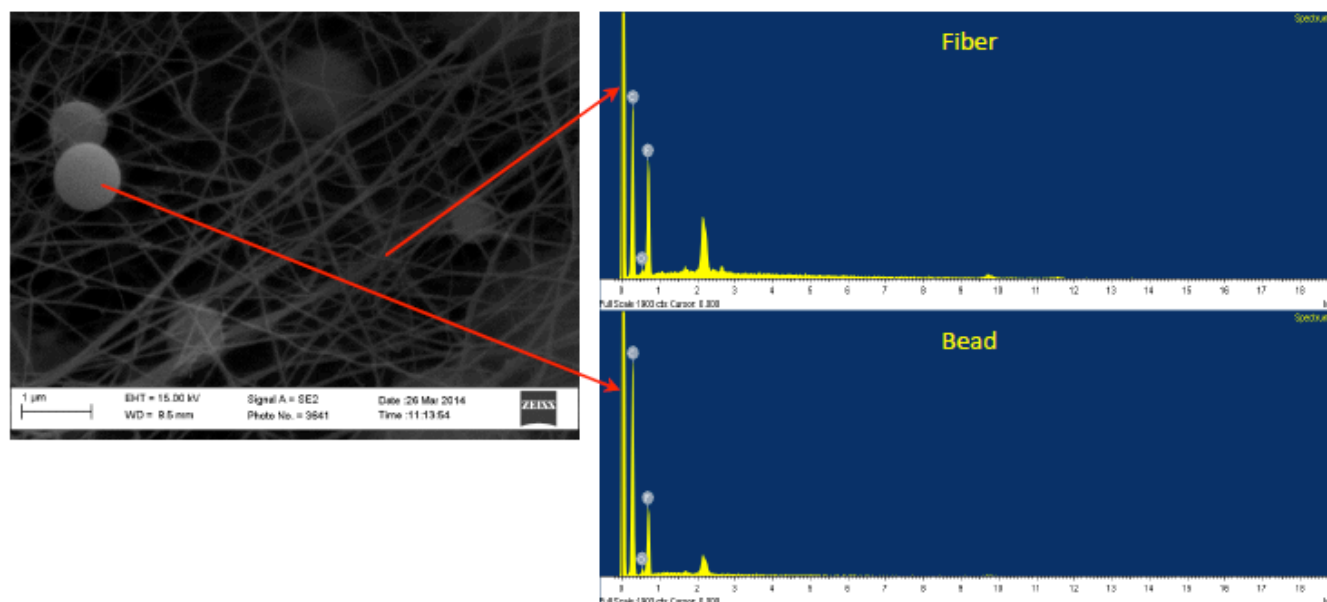


**Figure 3:** EDX results of fibers and beads of PVdF/PVP with 4wt% carbon black.

nanofibers are nanosize, and fiber diameters are in the range of 100 to 200nm. A good combination of PVdF/PVP and carbon black nanopowders is observed in all samples. However, some round-shaped beads were formed during electrospinning, especially in the 4wt% carbon black, which may be due to the high carbon loadings in the polymeric solution.

EDX spectroscopy was applied to determine the composition of fibers and beads in the structure. Figure 3 shows the EDX spectroscopy results of beads and fibers, indicating that both consist of carbon (C) and oxygen (O) elements, and the EDX scan on the surface of the beads and fibers shows that the carbon concentration in the beads is higher than the carbon concentration in the fibers. However, the fibers presented a higher fluorine (F) concentration. Surface EDX elemental data also provided information on the distribution of C, F and O atoms in the fibers and beads. The loading percentage may create some beads during the electrospinning process. EDX results of the electrospun PVdF/PVP nanocomposite fibers and beads provided in Table 1 confirm the agglomeration of carbon particles.

**Table 1: EDX Results of Electrospun PVdF/PVP Nanocomposite Fibers and Beads**

Element	Fiber Composition (%)	Bead Composition (%)
Carbon (C)	65.54	73.84
Oxygen (O)	2.10	3.13
Fluoride (F)	32.36	23.03

### 3.2. FTIR and Raman Spectroscopy Results

In this study, the chemical structures of electrospun PVdF/PVP nanofibers were characterized by FTIR to specify the spectral regions. The FTIR spectra of PVdF/PVP nanofibers incorporated with carbon black powders were recorded using a Thermal Nicolet Avatar 360 IR spectrometer in the range of 4,000 to 400 $\text{cm}^{-1}$ . Results of pure PVdF, PVP, and carbon black materials are shown in Figure 4.

In the FTIR spectra of pure PVdF, the corresponding crystalline  $\alpha$ -phase peak was observed at 490 $\text{cm}^{-1}$ , representing the wagging and bending vibrations of the  $\text{CF}_2$  group [23]. Other peaks of the crystalline  $\alpha$ -phase were also detected at 615 and 763 $\text{cm}^{-1}$ . The absorption band at 763 $\text{cm}^{-1}$  is related to a rocking vibration [24]. The band at 615 $\text{cm}^{-1}$  shows a mixed mode of C-C-C skeletal vibration and  $\text{CF}_2$  vibration [24, 25]. A characteristic  $\beta$ -phase peak at 840 $\text{cm}^{-1}$  is assigned to a mixed mode of  $\text{CH}_2/\text{CF}_2$  stretching vibrations [25, 26]. The band at 745 $\text{cm}^{-1}$  is defined as a rocking mode. The very strong band appearing at 1,184 $\text{cm}^{-1}$  is mainly formed by the  $\text{CF}_2$  symmetric stretching mode [26]. The  $\text{CH}_2$  group is described in two frequencies between 2,800 and 3,100 $\text{cm}^{-1}$ . Peaks at 1,435, 2,978 and 3,016 $\text{cm}^{-1}$  confirm stretching of the  $\text{CH}_2$  group [24]. The symmetric and asymmetric stretching vibrations of the  $\text{CH}_2$  group are located at 3,016 $\text{cm}^{-1}$  and 2,978 $\text{cm}^{-1}$ , respectively. Asymmetric vibrations are generally stronger than symmetric vibrations since the

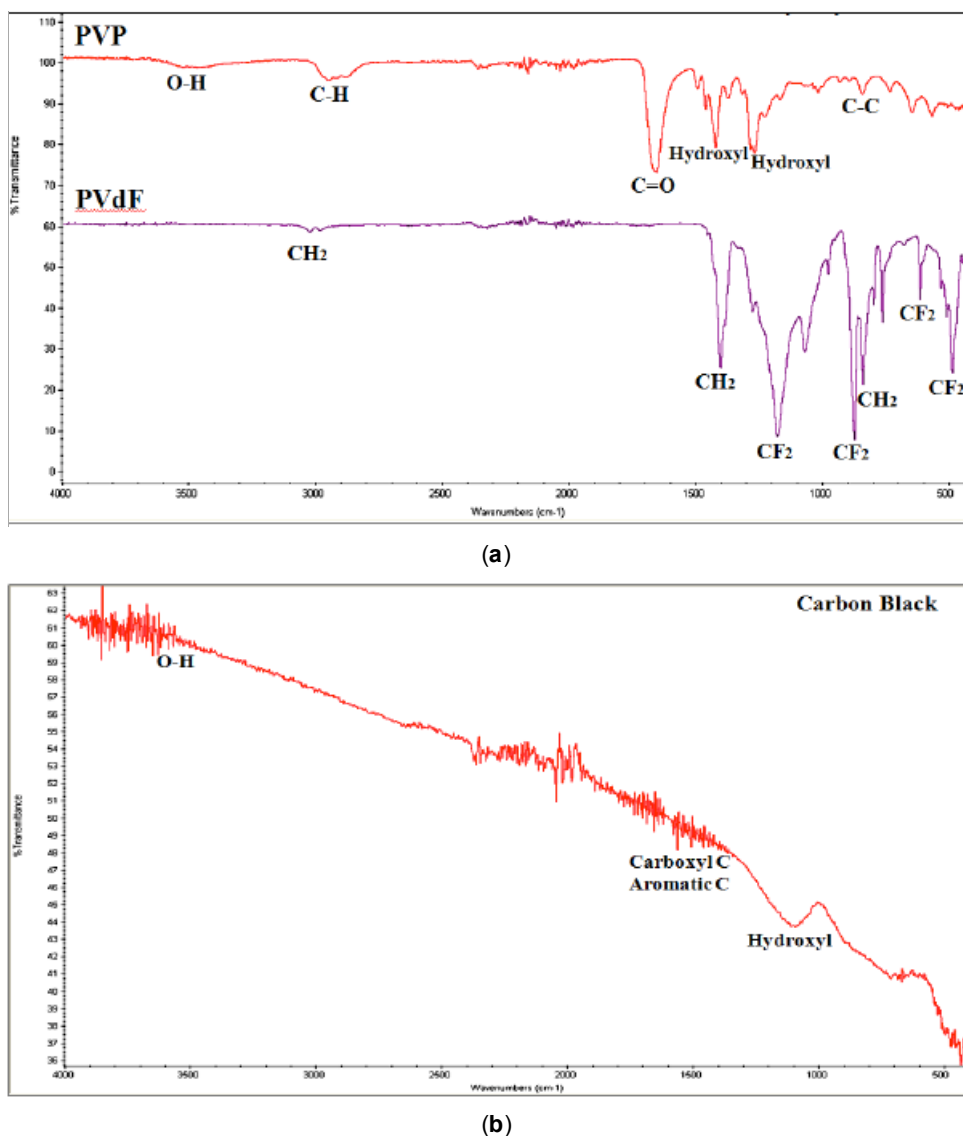


**Figure 4:** FTIR spectrum: (a) pure PVP and PVdF, and (b) carbon black.

asymmetric situation leads to minor changes in dipole moment [24, 26].

The FTIR spectrum of PVP displayed strong peaks at 1,286 and 1,447cm<sup>-1</sup>, which are attributed to the bending vibrations of the hydroxyl group. The band at 2,900cm<sup>-1</sup> is due to the C-H stretching vibration [27]. The C=O vibration groups show a prominent peak at 1,663cm<sup>-1</sup> [28]. The infrared peak at 760cm<sup>-1</sup> is attributed to C-C bending. The broad peak of O-H stretching is observed at 3,500cm<sup>-1</sup> [27].

The FTIR spectra of carbon black show band overlapping, which is attributed to carboxyl C and aromatic C between 1,700 and 1,500cm<sup>-1</sup>. The presence of the phenolic hydroxyl group is considered to be in the range of 1,000 to 1,200cm<sup>-1</sup>. Carbon black appears at the low absorbance of O-H stretching

vibrations around 3,400 to 3,450cm<sup>-1</sup>, probably from the phenolic groups [29]. Figure 5 illustrates the FTIR spectra of PVdF/PVP nanofibers by adding different percentages of carbon black nanopowders.

All nanofiber samples showed CF<sub>2</sub> and CH<sub>2</sub> groups from 490 to 1435cm<sup>-1</sup> and C=O vibration groups at 1,663cm<sup>-1</sup> related to PVdF and PVP spectrums, respectively. The presence of 0.5, 1, and 2wt% of carbon black resulted in sharp peaks of C≡N and C≡C bondings at 2,300 to 2,400cm<sup>-1</sup>. CH<sub>2</sub> group stretching was identified in the range of 2,978 to 3,016cm<sup>-1</sup> to all PVdF/PVP nanofibers; however, a prominent peak was shown for the 4wt% of carbon black. A strong peak at 3,500 to 3,700cm<sup>-1</sup> in the 4wt% of carbon black samples is attributed to the O-H group. Surface functional groups—O-containing and N-containing groups—in the samples can considerably enhance the

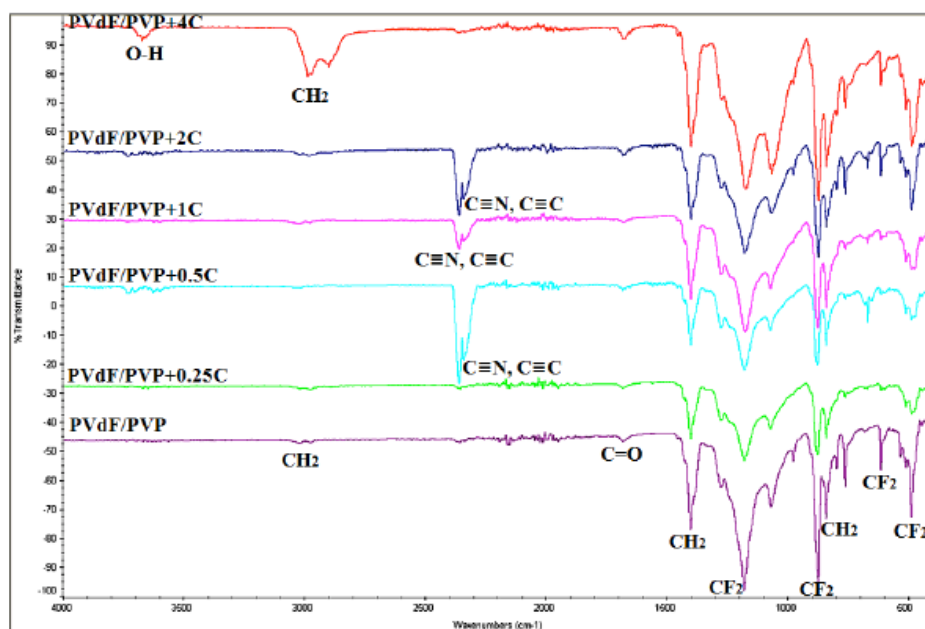


**Figure 5:** FTIR spectra of PVdF/PVP nanofibers as a function of different percentages of carbon black nano inclusions.

total capacitance values through additional Faradaic reactions called the pseudocapacitance effect [30-34].

Raman spectra were recorded by employing a HORIBA Scientific Xplora spectrometer in the range of 400 to 4,000 $\text{cm}^{-1}$ . A laser operating at 542nm radiation was used as the excitation source. Raman spectroscopy is the most suitable, simple, and quick method to provide details about molecular structures. In contrast to FTIR, Raman spectroscopy data provide more information for the low bands, which are not

visible with FTIR analysis alone. Raman spectra of PVdF have been studied to observe different phases that are not identified with FTIR. Raman spectroscopy results confirmed FTIR observations [35, 36]. The Raman spectra of electrospun PVdF/PVP nanofiber are shown in Figure 6. As can be seen, most of the bands correspond to the  $\alpha$ -phase of PVdF.

The strong and intense band at 799 $\text{cm}^{-1}$  is related to the  $\text{CH}_2$  rocking vibration [35]. Raman scattering around 810 $\text{cm}^{-1}$  shows the  $\gamma$ -phase of PVdF, which

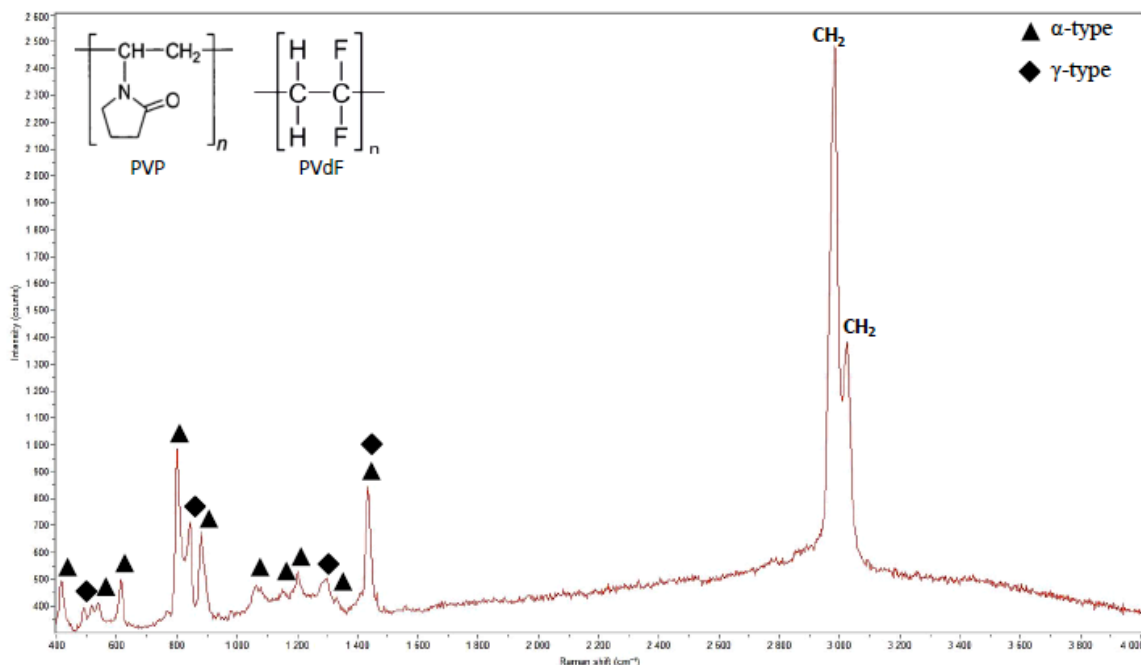


**Figure 6:** Raman spectra of PVdF/PVP nanofiber.

gives a high frequency for the liberation lattice mode due to the strong molecular force [37]. The peak at  $442\text{cm}^{-1}$  is assigned to the  $\text{CF}_2$  rocking mode of the  $\alpha$ -phase. The intense Raman peak at  $878\text{cm}^{-1}$  is due to the symmetric stretching vibration of the C-C bond [38]. The weak bonding at 490 and  $1,280\text{cm}^{-1}$  corresponds to the  $\gamma$ -phase of PVdF, whereas the peak at  $893\text{cm}^{-1}$  is attributed to the  $\alpha$ -phase. The strong band at 1,440 is a mixture of  $\alpha$ -phase and  $\gamma$ -phase crystals [39]. The presence of PVP in the PVdF matrix shows strong peaks at 2,980 and  $3,020\text{cm}^{-1}$ , which are attributed to the asymmetric stretching of  $\text{CH}_2$  chains [40].

### 3.3. XRD Analysis

X-ray results were collected with a Philips X'Pert system (Cu K  $\alpha$  radiation,  $\lambda = 1.5418 \text{ \AA}$ ). Figure 7 shows the wide-angle X-ray diffractometry (WAXD) diagram of annealed pure PVdF/PVP and annealed PVdF/PVP with 4wt% carbon black fibers.

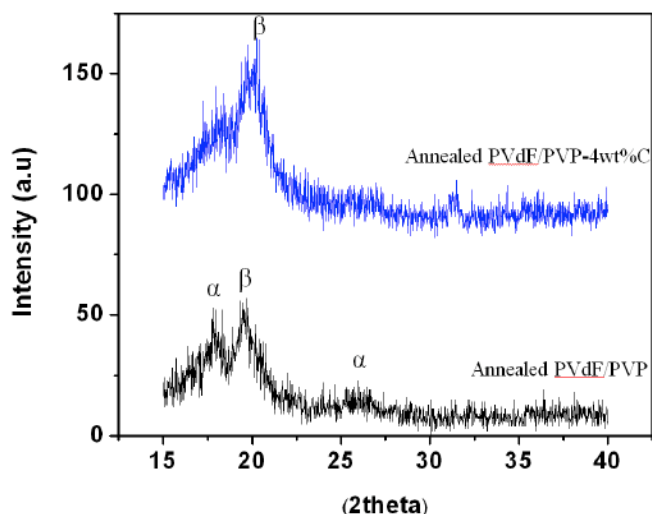


**Figure 7:** WAXD pattern of annealed pure PVdF/PVP and annealed PVdF/PVP with 4wt% carbon black nanofibers.

No peaks were detected in the pure PVdF/PVP samples without annealing. As can be seen, the diffraction patterns of the PVdF/PVP electrospun fibers displayed two peaks at 2 theta around  $18^\circ$  and  $20^\circ$ , corresponding to  $\alpha$ -phase and  $\beta$ -phase crystals, respectively [41-43]. The small peak around  $27^\circ$  is observed only for the  $\alpha$ -phase [43]. Adding 4wt% of carbon black exhibited a single peak around  $21^\circ$ , corresponding to (110) and (200) reflection of the  $\beta$ -phase crystal of PVdF, and the  $\alpha$ -phase showed low intensity [44].

In addition, PVdF/PVP fibers with 4wt% carbon black showed higher intensities of the  $\beta$ -phase peak than pure PVdF/PVP, and 2 theta of this form also

slightly shifted to higher angles. The addition of carbon black resulted in further enhancement of the  $\beta$ -phase content of PVdF. Moreover, the XRD spectra in both samples displayed an amorphous structure of the fibers.

## 4. CONCLUSIONS

Electrospun nanofibers of PVdF/PVP incorporated with different percentages of carbon black nanopowders were fabricated, characterized and analyzed in detail. SEM images showed that all the PVdF/PVP nanofibers were at nanosize (between 100 and 200nm). EDX elemental data also provided information on the distribution of C, F, and O atoms in the fibers and beads, which indicates a high concentration of carbon atoms in the beads of the fibers. FTIR results displayed some functional oxygen and nitrogen groups in samples that can considerably enhance the total capacitance values through additional Faradaic reactions called the pseudo-capacitance effect. Raman spectroscopy spectra also displayed different forms of PVdF. Wide XRD diagrams of annealed PVdF/PVP samples confirmed the presence of  $\alpha$ -phase and  $\beta$ -phase crystals. However, the addition of carbon black further enhanced the  $\beta$ -phase content of PVdF. Overall; this study may open up new possibilities to produce new separators for the future applications of supercapacitors.

## ACKNOWLEDGMENT

The authors gratefully acknowledge the Kansas NSF EPSCoR (#R51243/700333), and Wichita State University for the financial and technical support of this work.

## REFERENCES

- [1] Xu B, Yue S, Sui Z, Zhang X, Hou S, Cao G, et al. What is the choice for supercapacitors: Graphene or graphene oxide. *Energy Environ Sci* 2011; 4: 2826-2830. <http://dx.doi.org/10.1039/c1ee01198g>
- [2] Aravindan V, Cheah YL, Mak W F, Wee G, Chowdari B V R and Madhavi S. Fabrication of high energy-density hybrid supercapacitors using electrospun V2O5 nanofibers with a self-supported carbon nanotube network. *Chem Plus Chem* 2012; 77: 570-575. <http://dx.doi.org/10.1002/cplu.201200023>
- [3] Wee G, Soh HZ, Cheah YL, Mhaisalkar SG and Srinivasan M. Synthesis and electrochemical properties of electrospun V2O5 nanofibers as supercapacitor electrodes. *J Mater Chem* 2010; 20: 6720-6725. <http://dx.doi.org/10.1039/c0jm00059k>
- [4] Kim BH, Yang KS, Woo HG and Oshida K. Supercapacitor performance of porous carbon nanofiber composites prepared by electrospinning polymethylhydrosiloxane (PMHS)/polyacrylonitrile (PAN) blend solutions. *Synth Met*

- 2011; 161: 1211-1216.  
<http://dx.doi.org/10.1016/j.synthmet.2011.04.005>
- [5] Li J, Liu EH, Li W, Meng XY and Tan ST. Nickel/carbon nanofibers composite electrodes as supercapacitors prepared by electrospinning. *J Alloys Compd* 2009; 478: 371-374.  
<http://dx.doi.org/10.1016/j.jallcom.2008.11.024>
- [6] Zhou Z, Lai C, Zhang L, Qian Y, Hou H, Reneker D H, et al. Development of carbon nanofibers from aligned electrospun polyacrylonitrile nanofiber bundles and characterization of their microstructural, electrical, and mechanical properties. *Polym J* 2009; 50: 2999-3006.  
<http://dx.doi.org/10.1016/j.polymer.2009.04.058>
- [7] Kim C, Kim JS, Kim SJ, Lee WJ and Yang KS. Supercapacitors prepared from carbon nanofibers electrospun from polybenzimidazol. *J Electrochem Soc* 2004; 151(5): A769-A773.  
<http://dx.doi.org/10.1149/1.1695380>
- [8] Shiang T, Gene S, Wei W and Ashutosh T. Carbonized wood for supercapacitor electrodes. *Electrochem Solid-State Lett* 2014; 2(5): M25-M28.
- [9] Zhang L and Zhao XS. Carbon-based materials as supercapacitor electrodes. *Chem Soc Rev* 2009; 38: 2520-2531.  
<http://dx.doi.org/10.1039/b813846j>
- [10] Xu B, Peng L, Wang G, Cao G and Wu F. Easy synthesis of mesoporous carbon using nano-CaCO<sub>3</sub> as template. *Carbon* 2010; 48: 2377-2380.  
<http://dx.doi.org/10.1016/j.carbon.2010.03.003>
- [11] Heon M, Liofland S, Applegate J, Nottle R, Cortes E, Hettlinger JD, et al. Continuous carbide-derived carbon films with high volumetric capacitance. *Energy Environ Sci* 2011; 4: 135-138.  
<http://dx.doi.org/10.1039/C0EE00404A>
- [12] Zhu Y, Murali S, Stoller MD, Ganesh KJ, Cai W, Ferreira PJ, et al. Carbon-based supercapacitors produced by activation of graphene. *Science* 2011; 332: 1537-1541.  
<http://dx.doi.org/10.1126/science.1200770>
- [13] Khan WS, Asmatulu R and El-Tabey MM. Dielectric properties of electrospun PVP and PAN nanocomposite fibers. *J Nanotech Eng Med* 2010; 1: 1-6.  
<http://dx.doi.org/10.1115/1.4002533>
- [14] Khan WS, Asmatulu R, Lin YH, Chen YY and Ho J. Electrospun polyvinylpyrrolidone-based nanocomposite fibers containing (Ni<sub>0.6</sub>Zn<sub>0.4</sub>)Fe<sub>2</sub>O<sub>4</sub>. *J Nanotech* 2012; 2012: 1-5.  
<http://dx.doi.org/10.1155/2012/138438>
- [15] Khan W S, Asmatulu R, Ceylan M and Jabbarnia A. Recent progress on conventional and non-conventional electrospinning process. *Fibers Polym* 2013; 14(8): 1235-1247.  
<http://dx.doi.org/10.1007/s12221-013-1235-8>
- [16] Kim C, Yang KS and Lee WJ. The use of carbon nanofiber electrodes prepared by electrospinning for electrochemical supercapacitors. *Electrochem Solid-State Lett* 2004; 7(11): A397-A399.  
<http://dx.doi.org/10.1149/1.1801631>
- [17] Yoon SJ, Arakawa K and Uchino M. Development of an energy harvesting damper using PVDF film. *Int J Energy Res* 2015; 39: 1545-1553.  
<http://dx.doi.org/10.1002/er.3357>
- [18] Zheng J, He A, Li J and Han CC. Polymorphism control of poly (vinylidene fluoride) through electrospinning. *Macromol Rapid Commun* 2007; 28: 2159-2162.  
<http://dx.doi.org/10.1002/marc.200700544>
- [19] Dillon DR, Tenneti KK, Li CY, Ko FK, Sics I and Hsiao BS. On the structure and morphology of polyvinylidene fluoride-nanoclay nanocomposites. *Polym J* 2006; 47: 1678-1688.  
<http://dx.doi.org/10.1016/j.polymer.2006.01.015>
- [20] Huang ZB, Gao DS, Li ZH, Lei GT and Zhou J. P(VDF-HFP)-based polymer electrolytes prepared by high-voltage electrospinning technology. *Acta Chim Sinica* 2007; 65: 1007-1011.
- [21] Pandolfo AG, and Hollenkamp AF. Carbon properties and their role in supercapacitors. *J Power Sources* 2006; 157: 11-27.  
<http://dx.doi.org/10.1016/j.jpowsour.2006.02.065>
- [22] Beck F, Dolata M, Grivei E and Probst N. Electrochemical supercapacitors based on industrial carbon blacks in aqueous H<sub>2</sub>SO<sub>4</sub>. *J Appl Electrochem* 2001; 31(8): 845-853.  
<http://dx.doi.org/10.1023/A:1017529920916>
- [23] Hilczer B and Kulek J. The effect of dielectric heterogeneity on pyroelectric response of PVDF. *IEEE Trans Dielect Elec Insulation* 1998; 5(1): 45-50.  
<http://dx.doi.org/10.1109/94.660762>
- [24] Betz N, Le Moel A, Balanzat E, Ramillon JM, Lamotte J, Gallas JP, et al. A FTIR study of PVDF irradiated by means of swift heavy ions. *J Polym Sci Part B: Polym Phys* 1994; 32: 1493-1502.  
<http://dx.doi.org/10.1002/polb.1994.090320821>
- [25] Mattsson B, Ericson H, Torell LM and Sundholm F. Micro-Raman investigations of PVDF-based proton-conducting membranes. *J Polym Sci Part A: Polym Chem* 1999; 37: 3317-3327.  
[http://dx.doi.org/10.1002/\(SICI\)1099-0518\(19990815\)37:16<3317::AID-POLA30>3.0.CO;2-#](http://dx.doi.org/10.1002/(SICI)1099-0518(19990815)37:16<3317::AID-POLA30>3.0.CO;2-#)
- [26] Bharti V, Kaura T and Nath R. Ferroelectric hysteresis in simultaneously stretched and corona-poled PVDF films. *IEEE Trans Dielect Elec Insulation* 1997; 4(6): 738-741.  
<http://dx.doi.org/10.1109/94.654689>
- [27] Sivaiah K, Rudramadevi BH and Buddhudu S. Structural, thermal and optical properties of Cu<sup>2+</sup> and Co<sup>2+</sup>: PVP polymer films. *Indian J Pure Appl Phys* 2010; 48: 658-662.
- [28] Tu W. Study on the interaction between polyvinylpyrrolidone and platinum metals during the formation of the colloidal metal nanoparticles. *Chin J Polym Sci* 2008; 26(1): 23-29.  
<http://dx.doi.org/10.1142/S0256767908002625>
- [29] Lehmann J, Liang BQ, Solomon D, Lerotic M, Luizao F, Kinyangi J, et al. Near-edge X-ray absorption fine structure (NEXAFS) spectroscopy for mapping nano-scale distribution of organic carbon forms in soil: Application to black carbon particles. *Global Biogeochem Cycles* 2005; 19: 1-12.  
<http://dx.doi.org/10.1029/2004GB002435>
- [30] Raymundo-Pinero E, Cadek M and Beguin F. Tuning carbon materials for supercapacitors by direct pyrolysis of seaweeds. *Adv Funct Mater* 2009; 19: 1032-1039.  
<http://dx.doi.org/10.1002/adfm.200801057>
- [31] Hsieh CT and Teng H. Influence of oxygen treatment on electric double-layer capacitance of activated carbon fabrics. *Carbon* 2002; 40: 667-674.  
[http://dx.doi.org/10.1016/S0008-6223\(01\)00182-8](http://dx.doi.org/10.1016/S0008-6223(01)00182-8)
- [32] Xu B, Wu F, Wang F, Chen S, Cao G and Yang Y. Single-walled carbon nanotubes as electrode materials for supercapacitors. *Chin J Chem* 2006; 24: 1505-1508.  
<http://dx.doi.org/10.1002/cjoc.200690284>
- [33] Bao Q, Bao S, Li C, Qi X, Pan C, Zang J, et al. Supercapacitance of solid carbon nanofibers made from ethanol flames. *J Phys Chem C* 2008; 112: 3612-3618.  
<http://dx.doi.org/10.1021/jp710420k>
- [34] Hatori H, Zhu ZH and Lu GQ. Nitrogen-enriched nonporous carbon electrodes with extraordinary supercapacitance. *Adv Funct Mater* 2009; 19: 1800-1809.  
<http://dx.doi.org/10.1002/adfm.200801100>
- [35] Nallasamy P and Mohan S. Vibrational spectroscopic characterization of form II poly (vinylidene fluoride). *Indian J Pure Appl Phys* 2005; 43: 821-827.
- [36] Rodriguez-Cabello JC, Merino JC and Pastor JM. Rheo-optical FT-Raman study of uniaxially stretched



- poly(vinylidene fluoride). *J Macromol Chem Phys* 1995; 196: 815-824.  
<http://dx.doi.org/10.1002/macp.1995.021960311>
- [37] Kobayashi M, Tashiro K and Tadokoro H. Molecular vibrations of three crystal forms of poly (vinylidene fluoride). *Macromol* 1975; 8(2): 158-170.  
<http://dx.doi.org/10.1021/ma60044a013>
- [38] A Kuptsov H and Zhizhin GN. *Handbook of Fourier Transform Raman and Infrared Spectra of Polymer*. Elsevier: Amsterdam 1998.
- [39] Boccaccio T, Bottino A, Capannelli G and Piaggio P. Characterization of PVDF membranes by vibrational spectroscopy. *J Membrane Sci* 2002; 210(2): 315-329.  
[http://dx.doi.org/10.1016/S0376-7388\(02\)00407-6](http://dx.doi.org/10.1016/S0376-7388(02)00407-6)
- [40] Borodko Y, Habas SE, Koebel M, Yang P, Frei H and Somorjai GA. Probing the interaction of poly(vinylpyrrolidone) with platinum nanocrystals by UV-Raman and FTIR. *J Phys Chem B* 2006; 110: 23052-23059.  
<http://dx.doi.org/10.1021/jp063338+>
- [41] Nasir M, Matsumoto H, Minagawa M, Tanioka A, Danno T and Horibe H. Preparation of porous PVDF nanofiber from PVDF/PVP blend by electrospray deposition. *Polym J* 2007; 39(10): 1060-1064.  
<http://dx.doi.org/10.1295/polymj.PJ2007037>
- [42] Chanmal CV and Jog JP. Electrospun PVDF/BaTiO<sub>3</sub> nanocomposites: Polymorphism and thermal emissivity studies. *Int J Plast Technol* 2011; 15: S1-S9.  
<http://dx.doi.org/10.1007/s12588-011-9001-5>
- [43] Choi SW, Kim JR, Ahm YR, Jo SM and Cairns EJ. Characterization of electrospun PVdF fiber-based polymer electrolytes. *Chem Mater* 2007; 19: 104-115.  
<http://dx.doi.org/10.1021/cm060223+>
- [44] Yang Y, Centrone A, Chen L, Simeon F, Hatton TA and Rutledge GC. Highly porous electrospun polyvinylidene fluoride (PVDF)-based carbon fiber. *Carbon* 2011; 49: 3395-3403.  
<http://dx.doi.org/10.1016/j.carbon.2011.04.015>

Received on 08-11-2015

Accepted on 22-01-2016

Published on 09-02-2016

DOI: <http://dx.doi.org/10.15377/2410-4701.2015.02.02.3>

© 2015 Jabbarnia and Asmatulu; Avanti Publishers.

This is an open access article licensed under the terms of the Creative Commons Attribution Non-Commercial License (<http://creativecommons.org/licenses/by-nc/3.0/>) which permits unrestricted, non-commercial use, distribution and reproduction in any medium, provided the work is properly cited.